CONF-951155-32

CRITERIA FOR PROGRESSIVE INTERFACIAL DEBONDING WITH FRICTION IN FIBER-REINFORCED CERAMIC COMPOSITES

CHUN-HWAY HSUEH
Metals and Ceramics Division, Oak Ridge National Laboratory, Oak Ridge, TN 37831

ABSTRACT

Criteria for progressive debonding at the fiber/matrix interface with friction along the debonded interface are considered for fiber-reinforced ceramic composites. The energy-based criterion is adopted to analyze the debond length, the crack-opening displacement, and the displacement of the composite due to interfacial debonding. The analytical solutions are identical to those obtained from the mismatch-strain criterion, in which interfacial debonding is assumed to occur when the mismatch in the axial strain between the fiber and the matrix reaches a critical value. Furthermore, the mismatch-strain criterion is found to bear the same physical meaning as the strength-based criterion.

INTRODUCTION

Bridging of matrix cracks by fibers, which debond from and slip frictionally against the matrix, is an important toughening mechanism in fiber-reinforced ceramic composites [1,2]. To analyze the toughening effect, a criterion for progressive debonding at the fiber/matrix interface accompanied by friction along the debonded interface is required. The loading stress on the fiber to initiate debonding (or the debond stress for a frictionless interface), σ_d, has been analyzed by using either the energy-based [3-6] or the strength-based criterion [7-9]. The effect of constant friction along the debonded interface on progressive debonding was analyzed recently by Nair [10] using the energy-based criterion and by Budiansky *et al.* [11] using the strength-based criterion. It is noted that refinement is required in Nair's analysis regarding the work done by load. An alternative debonding criterion was proposed recently in which debonding is assumed to occur when the mismatch in the axial strain between the fiber and the matrix reaches a critical value [12]. Based on this assumption, the solutions for progressive debonding have been obtained [13]. A question is raised as to whether the solutions obtained from the three debonding criteria mentioned above agree with each other.

The purpose of the present study is to address the above question. First, using the energy-based criterion, solutions for progressive debonding with a constant friction along the debonded interface are obtained by modifying Nair's analysis [10]. These solutions are then compared to those obtained from the mismatch-strain criterion. Finally, the physical meaning of the approach using the strength-based criterion is examined and compared to the mismatch-strain criterion.

THE ENERGY-BASED CRITERION

A unidirectional composite subjected to a tensile load in the direction parallel to the fiber axis is considered. Matrix cracking occurs perpendicular to the loading direction and is bridged by intact fibers, which exert a bridging stress, σ_o, to oppose crack-opening. This problem can be modeled by using a representative volume element shown in Fig. 1. A fiber with a radius, a, is located at the center of a coaxial cylindrical shell of matrix with an outer radius, b, such that a^2/b^2 corresponds to the volume fraction of fibers, V_f, in the composite (Fig. 1a). When the interface remains bonded, the composite is subjected to a tensile stress, $V_f\sigma_o$, and has a displacement, u_{bonded}, in the axial direction (Fig. 1b). In the presence of interfacial debonding, the bridging fiber is subjected to a tensile stress, σ_o, and the matrix is stress-free at the crack surface (Fig. 1c). Interfacial debonding and sliding occur along a length, h, with a frictional stress, τ, and the end of the debonding zone and the crack surface are located at z=0 and z=h, respectively. The half crack-opening displacement, u_o, is defined by the relative displacement between the fiber and the matrix at the crack surface (Fig. 1c). Also, compared to the composite without interfacial debonding (Fig. 1b), the composite with interfacial debonding has an additional displacement, u_{debond}, in the loading direction (Fig. 1c).

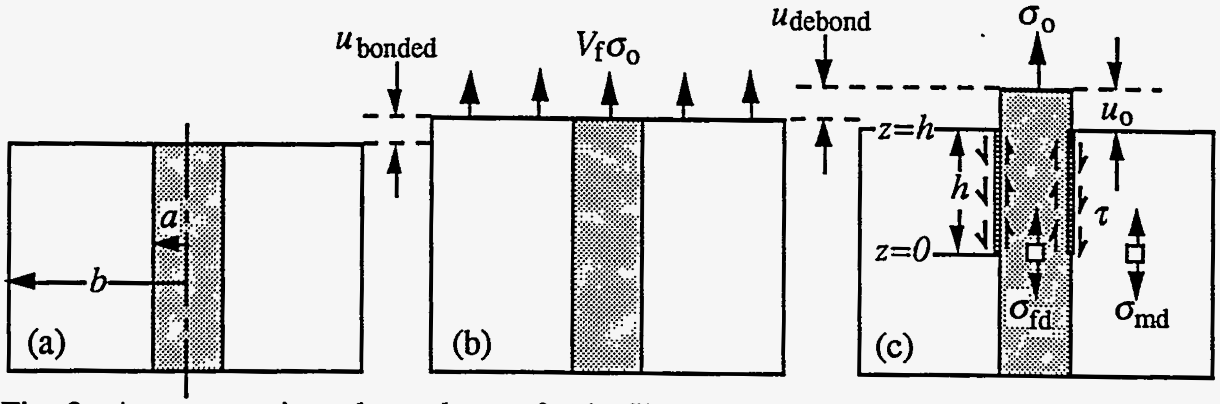

Fig. 2. A representative volume element for the fiber bridging problem: (a) prior to loading, (b) loading without interfacial debonding, and (c) loading with interfacial debonding. The half cracking opening displacement, u_o, and the displacement of the composite due to interfacial debonding, u_{debond}, are also shown.

Stresses in the fiber and the matrix

When the interface is bonded, the equilibrium axial stresses in the fiber and the matrix, σ_f and σ_m, satisfy both the equilibrium and the continuity conditions, such that

$$V_f\sigma_f + V_m\sigma_m = V_f\sigma_o \tag{1}$$

$$\frac{\sigma_f}{E_f} = \frac{\sigma_m}{E_m} \tag{2}$$

where V_m (=1-V_f) is the volume fraction of the matrix, and E_f and E_m are Young's moduli of the fiber and the matrix, respectively. Combination of Eqs. (1) and (2) yields

$$\sigma_f = \frac{V_f E_f \sigma_o}{E_c} \quad \text{(for bonded interface)} \tag{3a}$$

$$\sigma_m = \frac{V_f E_m \sigma_o}{E_c} \quad \text{(for bonded interface)} \tag{3b}$$

where $E_c = V_f E_f + V_m E_m$.

For a frictional interface, both σ_f and σ_m can be approximated to be independent of the radial coordinate [4,5], and Eq. (1) is satisfied. The axial stresses in the fiber and the matrix at the end of the debond length, σ_{fd} and σ_{md}, can be obtained from the stress transfer equation, such that

$$\sigma_{fd} = \sigma_o - \frac{2h\tau}{a} \tag{4a}$$

$$\sigma_{md} = \frac{2hV_f\tau}{aV_m} \tag{4b}$$

Solutions of σ_{fd} and σ_{md} are contingent upon the determination of h. With constant friction, the axial stress distributions in the fiber and the matrix, σ_f and σ_m, along the debond length are

$$\sigma_f = \sigma_{fd} + \frac{z(\sigma_o - \sigma_{fd})}{h} \qquad (o \le z \le h) \tag{5a}$$

$$\sigma_m = \left(1 - \frac{z}{h}\right)\sigma_{md} \qquad (o \le z \le h) \tag{5b}$$

Displacements

In the debonded region, the axial displacements resulting from the axial stresses described by Eqs. (5a) and (5b) are

$$w_f = \frac{z\sigma_{fd}}{E_f} + \frac{z^2(\sigma_o - \sigma_{fd})}{2hE_f} \qquad (o \le z \le h) \tag{6a}$$

$$w_m = \left(z - \frac{z^2}{2h}\right)\frac{\sigma_{md}}{E_m} \qquad (o \le z \le h) \tag{6b}$$

The half crack opening displacement, u_o ($=w_f$-w_m at $z=h$), becomes (Fig. 1c)

$$u_o = \frac{h\sigma_o}{E_f} - \frac{h^2 \tau E_c}{aV_m E_f E_m} \tag{7}$$

In the absence of interfacial debonding, the axial displacement in the composite, w_c, within a length, h, is (Fig. 1b)

$$w_c(h) = \frac{hV_f \sigma_o}{E_c} \tag{8}$$

Hence, the additional axial displacement of the composite due to debonding, u_{debond} ($=w_f(h)$-$w_c(h)$), becomes (Fig. 1c)

$$u_{debond} = \frac{hV_m E_m \sigma_o}{E_f E_c} - \frac{h^2 \tau}{aE_f} \tag{9}$$

Solutions of u_o and u_{debond} are also contingent upon the determination of the debond length, h, which is solved using the energy-based criterion as follows.

The debond length and related solutions

Based on the energy-based criterion, the following energy terms are involved: (1) U_e, the elastic strain energy in the composite, (2) U_s, the energy due to sliding at the debonded interface, (3) G_i, the energy release rate for interfacial debonding, and (4) W, the work done by the applied stress. The equilibrium debond length, h, can be determined by using the energy balance condition when the fiber is subjected to a loading stress, σ_o, the debond length is assumed to advance a distance dh, and the corresponding energy changes are dU_e, dU_s, dG_i and dW. The energy balance condition requires that

$$dW = dU_e + dU_s + dG_i \tag{10}$$

The above condition has been used by Nair [10] to derive the debond length; however, refinement of the derivation of dW is required. To determine the debond length, the present study summarizes the results for dU_e, dU_s and dG_i, and derives dW. However, a complete analysis of the debond length can be found elsewhere [14].

The results for dU_e, dU_s and dG_i are [10,14]:

$$dU_e = \frac{\pi a^2 V_m E_m}{2E_f E_c}\left(\sigma_o - \frac{2h\tau E_c}{aV_m E_m}\right)^2 dh \tag{11}$$

$$dU_s = 2\pi a\tau\left(\frac{h\sigma_o}{E_f} - \frac{2h^2\tau E_c}{aV_m E_f E_m}\right)dh \tag{12}$$

$$dG_i = 2\pi a G_i dh \tag{13}$$

With the bridging stress, σ_o, on the fiber, the work done due to interfacial debonding is $W=\pi a^2\sigma_o u_{debond}$. The change in the work done is hence

$$dW = \pi a^2 \sigma_o du_{debond} \tag{14}$$

It is noted that instead of using u_{debond}, u_o was incorrectly used in Nair's analysis in deriving dW. Substitution of Eq. (9) into Eq. (14) yields

$$dW = \pi a^2 \sigma_o\left(\frac{V_m E_m \sigma_o}{E_f E_c} - \frac{2h\tau}{aE_f}\right)dh \tag{15}$$

Substitution of Eqs. (11), (12), (13), and (15) into Eq. (10) yields

$$h = \frac{aV_m E_m}{2\tau E_c}\left[\sigma_o - 2\left(\frac{E_f E_c G_i}{aV_m E_m}\right)^{1/2}\right] \tag{16}$$

The stress required for initial debonding, σ_d, can be obtained from Eq. (16) by letting h=0, such that

$$\sigma_d = 2\left(\frac{E_f E_c G_i}{aV_m E_m}\right)^{1/2} \tag{17}$$

The solutions of u_o and u_{debond} can be obtained by substituting Eq. (16) into Eqs. (7) and (9), such that

$$u_o = \frac{aV_m E_m \sigma_o^2}{4E_f E_c \tau} - \frac{G_i}{\tau} \tag{18a}$$

$$u_{debond} = \frac{aV_m^2 E_m^2 \sigma_o^2}{4E_f E_c^2 \tau} - \frac{V_m E_m G_i}{E_c \tau} \tag{18b}$$

In the absence of interfacial bonding (i.e., G_i=0), equations (18a), and (18b) become

$$u_o = \frac{aV_m E_m \sigma_o^2}{4E_f E_c \tau} \tag{19a}$$

$$u_{debond} = \frac{aV_m^2 E_m^2 \sigma_o^2}{4E_f E_c^2 \tau} \tag{19b}$$

Equations (19a) and (19b) are identical to the displacements derived in the MCE [15] and the ACK [16] models, respectively. While u_{debond} is considered in the ACK model [16], u_o is considered in the MCE model [15].

The steady-state increase in toughness, ΔG, of the composite due to frictional bridging of the matrix crack by fibers is given by [11,17]

$$\Delta G = 2V_f \int_0^{u^*} \sigma_o du_{debond} \tag{20}$$

where u^* is the displacement of the composite due to interfacial debonding when the loading stress on the fiber, σ_o, reaches the fiber strength, σ_s. Substitution of Eq. (18b) into Eq. (20) yields

$$\Delta G = \frac{aV_f V_m{}^2 E_m{}^2}{3E_f E_c{}^2 \tau}\left(\sigma_s{}^3 - \sigma_d{}^3\right) \tag{21}$$

Hence, in order to achieve toughening effect (i.e., $\Delta G>0$), the fiber strength, σ_s, must be greater than the initial debond stress, σ_d.

COMPARISON WITH MISMATCH-STRAIN CRITERION

A simple debonding criterion has been proposed such that debonding occurs when the mismatch in the axial strain between the fiber and the matrix reaches a critical value [12]. Based on this criterion, solutions for progressive debonding with friction along the debonded interface have been derived [13] which are reviewed and compared with the present results as follows.

When the bridging stress reaches the initial debond stress, σ_d, debonding initiates at the crack surface, and the critical mismatch strain, ε_d, is

$$\varepsilon_d = \frac{\sigma_d}{E_f} \tag{22}$$

During subsequent loading (i.e., $\sigma_o>\sigma_d$), debonding extends underneath the surface, and the mismatch strain at the end of the debonding zone remains ε_d, such that

$$\varepsilon_d = \frac{\sigma_{fd}}{E_f} - \frac{\sigma_{md}}{E_m} \tag{23}$$

where σ_{fd} and σ_{md} are the axial stresses in the fiber and the matrix at the end of the debonding zone which satisfy the mechanical equilibrium condition described by Eq. (1). Combination of Eqs. (1), (22), and (23) yields

$$\sigma_{fd} = \frac{V_f E_f \sigma_o + V_m E_m \sigma_d}{E_c} \tag{24}$$

The debond length, h, can be obtained from Eqs. (4a) and (24), such that

$$h = \frac{aV_m E_m(\sigma_o - \sigma_d)}{2E_c \tau} \tag{25}$$

Equation (25) is identical to the results obtained from both the energy-based [Eq. (16)] and the strength-based [11] criteria. Both u_o and u_{debond} have also been derived using the mismatch-strain criterion [13], and they are identical to those obtained in the present study.

THE STRENGTH-BASED CRITERION

For the strength-based criterion, debonding occurs when the interfacial shear strength, τ_s, is reached. A difference has been noted between debonding at the crack surface and debonding underneath the crack surface [18]. Whereas the matrix is stress-free at the crack surface, it is subjected to axial stresses underneath the crack surface due to the stress transfer from the fiber to the matrix. Hence, the magnitude of the interfacial shear stress induced by a loading stress σ_d on the fiber at the crack surface is different from that induced by an axial stress σ_d in the fiber underneath the crack surface. Assuming that the axial stresses at the end of the debonding zone are σ_{fd} and σ_{md} respectively in the fiber and the matrix, the relation between σ_{fd} and σ_d can be derived using the strength-based criterion and this is shown as follows.

At the end of the debonding zone, the interfacial shear stress can be analyzed using the following procedures. First, tractions of $E_f\sigma_{md}/E_m$ and σ_{md} are imposed on the fiber and the matrix, respectively (Fig. 2a). This would result in a uniform axial strain σ_{md}/E_m in the composite, and no interfacial shear stress is induced. Then, a traction of $\sigma_{fd}-E_f\sigma_{md}/E_m$ is imposed on the fiber, and this would induce the interfacial shear stress (Fig. 2b). Combining the above two procedures, the tractions imposed on the fiber and the matrix are σ_{fd} and σ_{md} respectively (Fig. 2c). Hence, the interfacial shear stress at the end of the debonding zone is equivalent to that if a traction of $\sigma_{fd}-E_f\sigma_{md}/E_m$ is imposed on the fiber alone at the crack surface. To satisfy the debonding condition at the end of the debonding zone, the following relation is hence required:

$$\sigma_{fd}-\frac{E_f\sigma_{md}}{E_m}=\sigma_d \tag{26}$$

It is noted that Eq. (26) can also be obtained by combining Eq. (22) with Eq. (23). Hence, the strength-based criterion yields the same results as those using the mismatch-strain criterion.

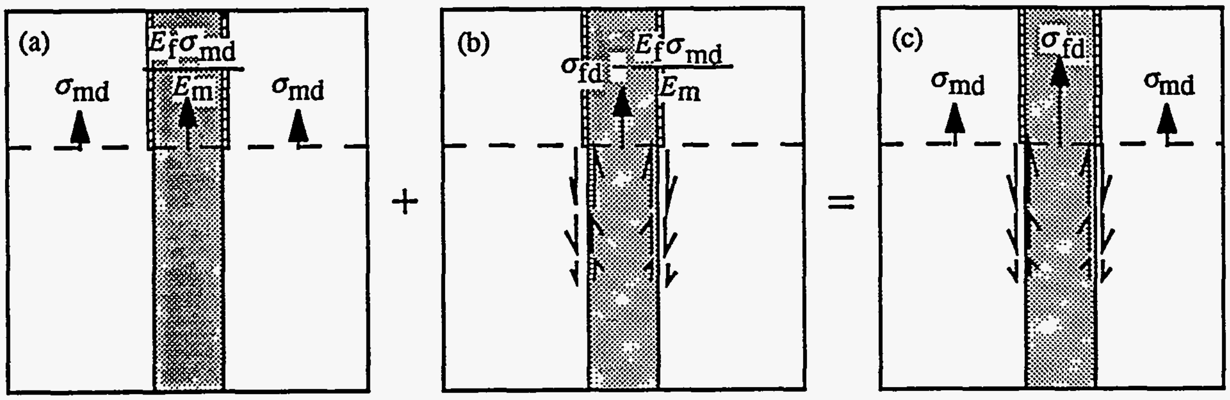

Fig. 2. The procedures in deriving the interfacial shear stress at the end of the debonding zone: (a) tractions of $E_f\sigma_{md}/E_m$ and σ_{md} are imposed on the fiber and the matrix, respectively, at the end of the debonding zone resulting a uniform axial strain in the composite, (b) a traction of $\sigma_{fd}-E_f\sigma_{md}/E_m$ is imposed on the fiber, and the interfacial shear stress is induced, (c) combination of the above two procedures results in the condition of tractions at the end of the debonding zone.

CONCLUSIONS

Using the energy-based criterion, progressive debonding at the fiber/matrix interface with friction along the debonded interface is analyzed for fiber-reinforced ceramic composites. It is noted that the displacement term involved in calculating the work done by load is the displacement of the composite due to interfacial debonding not the crack opening displacement. The present results for progressive debonding are identical to those obtained from the mismatch-strain criterion, in which interfacial debonding is assumed to occur when the mismatch in the axial strain between the fiber and the matrix reaches a critical value. Also, the mismatch-strain criterion is found to have the same physical meaning as the strength-based criterion.

ACKNOWLEDGMENTS

The author thanks Drs. P. F. Becher, E. Lara-Curzio and S. Raghuraman for reviewing the manuscript. Research sponsored jointly by the U.S. Department of Energy, Division of Materials Sciences, Office of Basic Energy Sciences, and Assistant Secretary for Energy Efficiency and Renewable Energy, Office of Industrial Technologies, Industrial Energy Efficiency Division and Continuous Fiber Ceramic Composites Program, under contract DE-AC05-84OR21400 with Lockheed Martin Energy Systems.

REFERENCES

1. A. G. Evans and R. M. McMeeking, *Acta Metall.*, **34**, 2435-2441 (1986).
2. P. F. Becher, C. H. Hsueh, P. Angelini and T. N. Tiegs, *J. Am. Ceram. Soc.*, **71**, 1050-1061 (1988).
3. C. Gurney and J. Hunt, *Proc. Roy. Soc. Lond.*, **A299**, 508-524 (1967).
4. Y. C. Gao, Y. W. Mai and B. Cotterell, *J. Appl. Math. and Phys. (ZAMP)*, **39**, 550-572 (1988).
5. J. W. Hutchinson and H. M. Jensen, *Mech. Materials*, **9**, 139-163 (1990)
6. C. H. Hsueh, *Mater. Sci. and Eng.*, **A159**, 65-72 (1992).
7. P. Lawrence, *J. Mater. Sci.*, **7**, 1-6 (1972).
8. A. Takaku and R. G. C. Arridge, *J. Phys. D: Appl. Phys.*, **6**, 2038-2047 (1973).
9. C. H. Hsueh, *Mater. Sci. and Eng.*, **A123**, 1-11 (1990).
10. S. V. Nair, *J. Am. Ceram. Soc.*, **73**, 2839-2847 (1990).
11. B. Budiansky, A. G. Evans, and J. W. Hutchinson, *Int. J. Solids Structures*, **32**, 315-328 (1995).
12. N. Shafry, D. G. Brandon and M. Terasaki, *Euro-Ceramics*, **3**, 3.453-457 (1989).
13. C. H. Hsueh, *J. Mater. Sci.*, **30**, 1781-1789 (1995).
14. C. H. Hsueh, submitted to *Acta Metall. Mater.*
15. D. B. Marshall, B. N. Cox, and A. G. Evans, *Acta Metall.*, **33**, 2013 (1985).
16. J. Aveston, G. A. Cooper, and A. Kelly, "The Properties of Fibre Composites," pp.15-26, Conference Proceedings, National Physical Laboratory, Guildford, IPC Science and Technology Press Ltd., (1971).
17. L. N. McCartney, *Proc. R. Soc. Lond.*, **A409**, 329-350 (1987).
18. J. K. Kim, C. Baillie, and Y. W. Mai, *J. Mater. Sci.*, **27**, 3143-3154 (1992).